

Supporting Information

Bright Green PhOLEDs Using Cyclometalated Iridium(III) Complexes with Bridging Oxamidato Ligands as Phosphorescent Dopants

Ahmed M'hamedi,[†] Mark A. Fox,[‡] Andrei S. Batsanov,[‡] Hameed A. Al-Attar,[§] Andrew P. Monkman[§]
and Martin R. Bryce^{*,‡}

[†] *Laboratory of Structure Determination, Development, and Application of Molecular Material, Department of Chemistry, University of Abdelhamid Ibn Badis BP 227, Mostaganem 27000 Algeria*

[‡] *Department of Chemistry, Durham University, South Road, Durham, DH1 3LE, UK*

[§] *Department of Physics, Durham University, South Road, Durham, DH1 3LE, UK*

Contents	Page
X-Ray crystallography	S2
Computations	S5
Mass Spectra	S12
Thermal analysis	S13
PhOLED data	S15
NMR Spectra	S16

X-ray crystallography

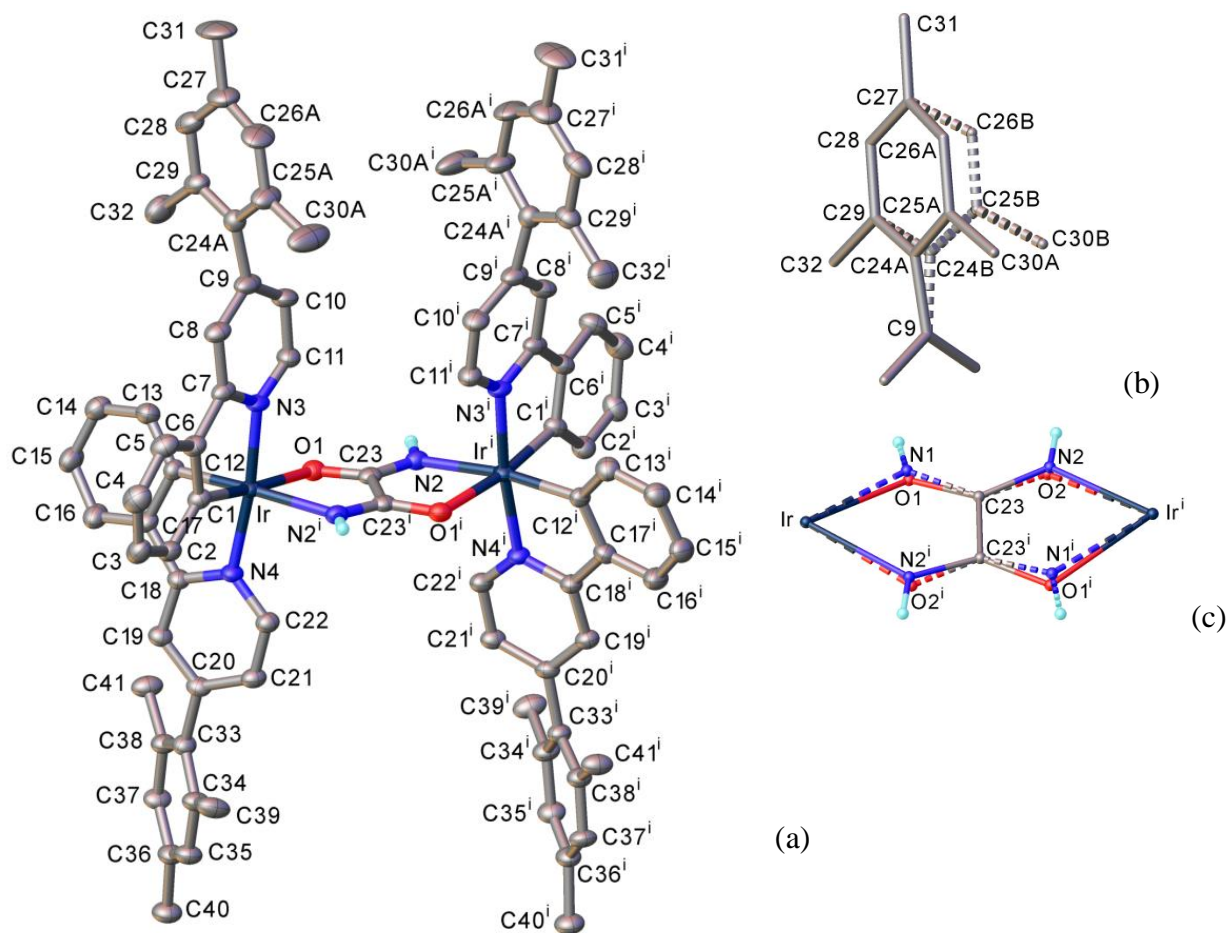


Figure S1. (a) Molecular structure of **5** (major component), (b) disorder of the mesityl group. (c) disorder of the bridging system. Here and below atomic displacement ellipsoids are shown at the 50% probability level. H atoms, except oxamidato, are omitted for clarity. Primed atoms were generated by a crystallographic twofold axis (transformation $\frac{1}{2} -x, y, 1-z$).

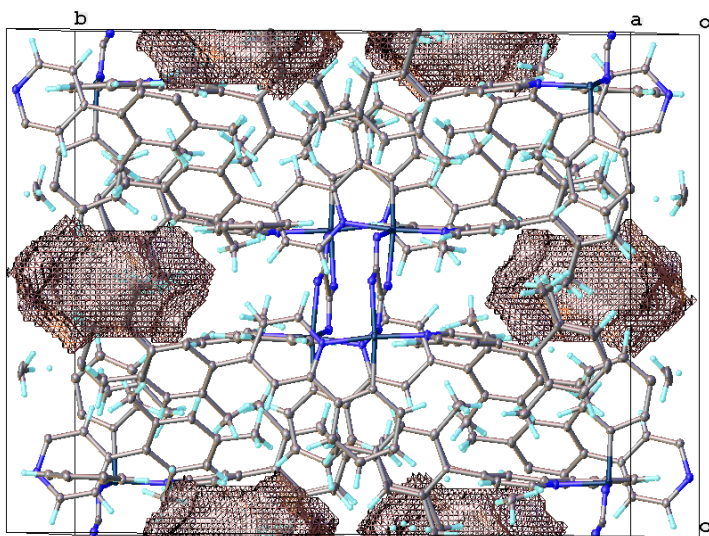


Figure S2. Solvent-accessible voids in the structure of **5**, presumably occupied by disordered hexane molecules.

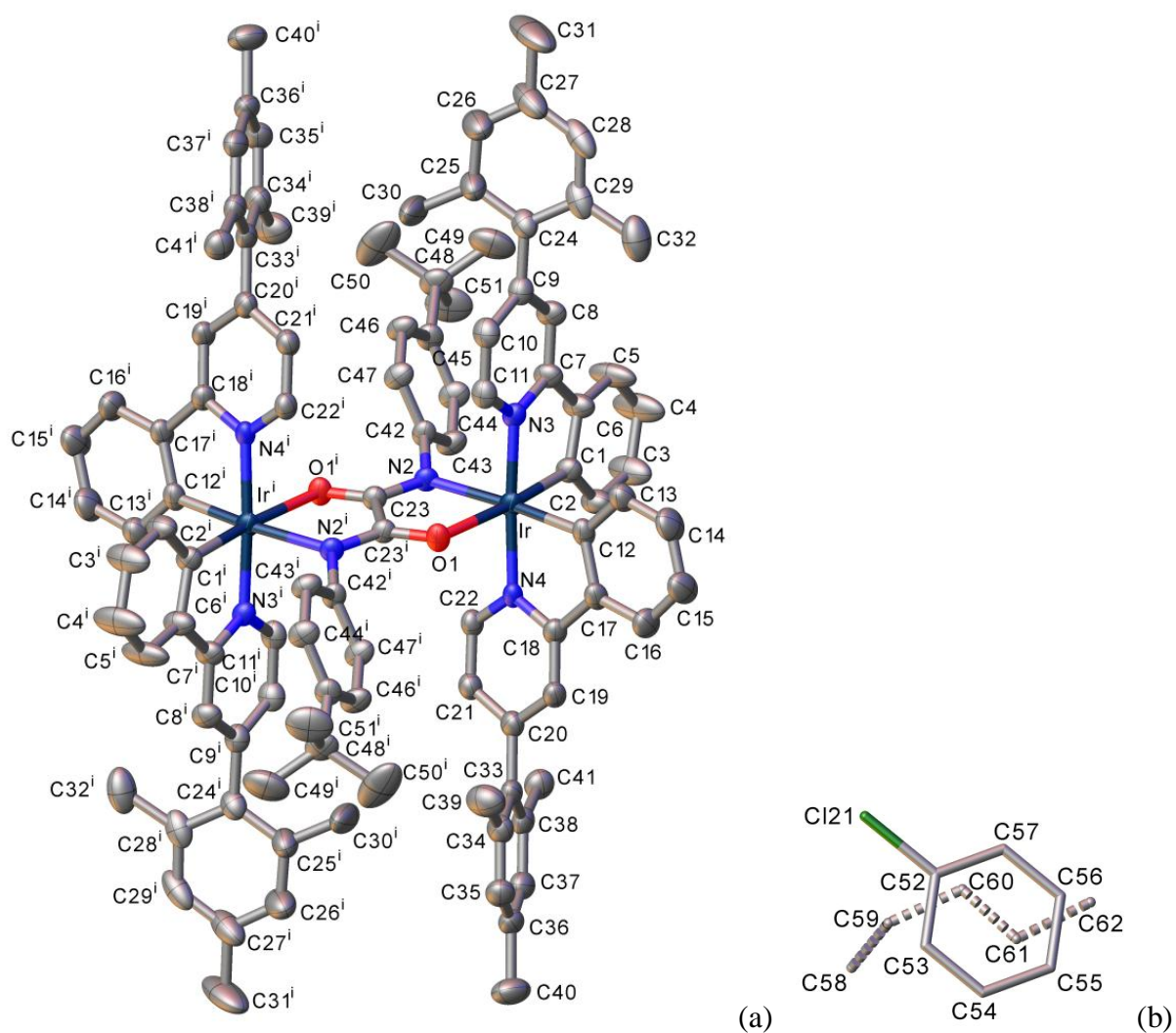


Figure S3. (a) Molecular structure of **6**; (b) disorder of chlorobenzene and pentane of crystallisation.

Table S1. Crystal data for **5** and **6**

Compound	5 ·hexane	6 ·PhCl·pentane
CCDC	1521969	1521970
Formula	C ₈₈ H ₈₈ Ir ₂ N ₆ O ₂	C ₁₁₃ H ₁₁₅ ClIr ₂ N ₆ O ₂
$D_{calc.}/\text{g cm}^{-3}$	1.546	1.420
μ/mm^{-1}	3.48	2.91
Formula Weight	1646.04	2008.95
Size/mm ³	0.05×0.03×0.02	0.08×0.06×0.05
T/K	100	120
Crystal System	monoclinic	triclinic
Space Group	$I2/a$ (#15)	$P-1$ (#2)
$a/\text{Å}$	15.122(3)	12.0305(6)
$b/\text{Å}$	24.292(4)	12.8786(6)
$c/\text{Å}$	19.265(5)	16.9004(8)
$\alpha/^\circ$	90	73.088(2)
$\beta/^\circ$	92.237(2)	70.775(2)
$\gamma/^\circ$	90	78.292(2)
$V/\text{Å}^3$	7071(3)	2348.8(2)
Z	4	1
$\Theta_{max}/^\circ$	29.6	26.4
Refls. total/unique	42109, 10354	37364, 9580
Reflections with $I > 2\sigma(I)$	7944	7606
R_{int}	0.044	0.051
Parameters/restraints	440, 10	619, 577
$\Delta\rho$ max/min, eÅ^{-3}	1.70, -1.87	1.36, -0.80
wR_2 (all data)	0.083	0.086
R_1 [$I > 2\sigma(I)$ data]	0.034	0.038

Computations

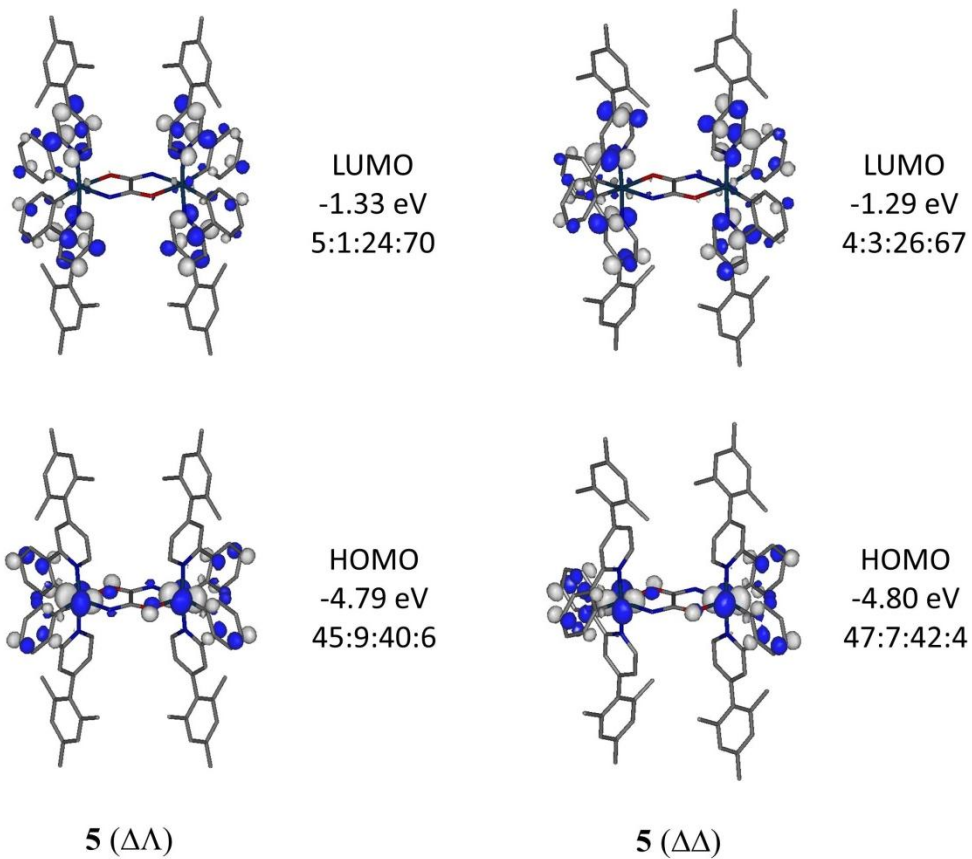


Figure S4. Frontier orbitals for **5**($\Delta\Delta$) and **5**($\Delta\Lambda$). Contour values are plotted at ± 0.035 e bohr⁻³. The Ir:bridge:phenyl:pyridyl ratios represent the atom/group MO contributions in percentages.

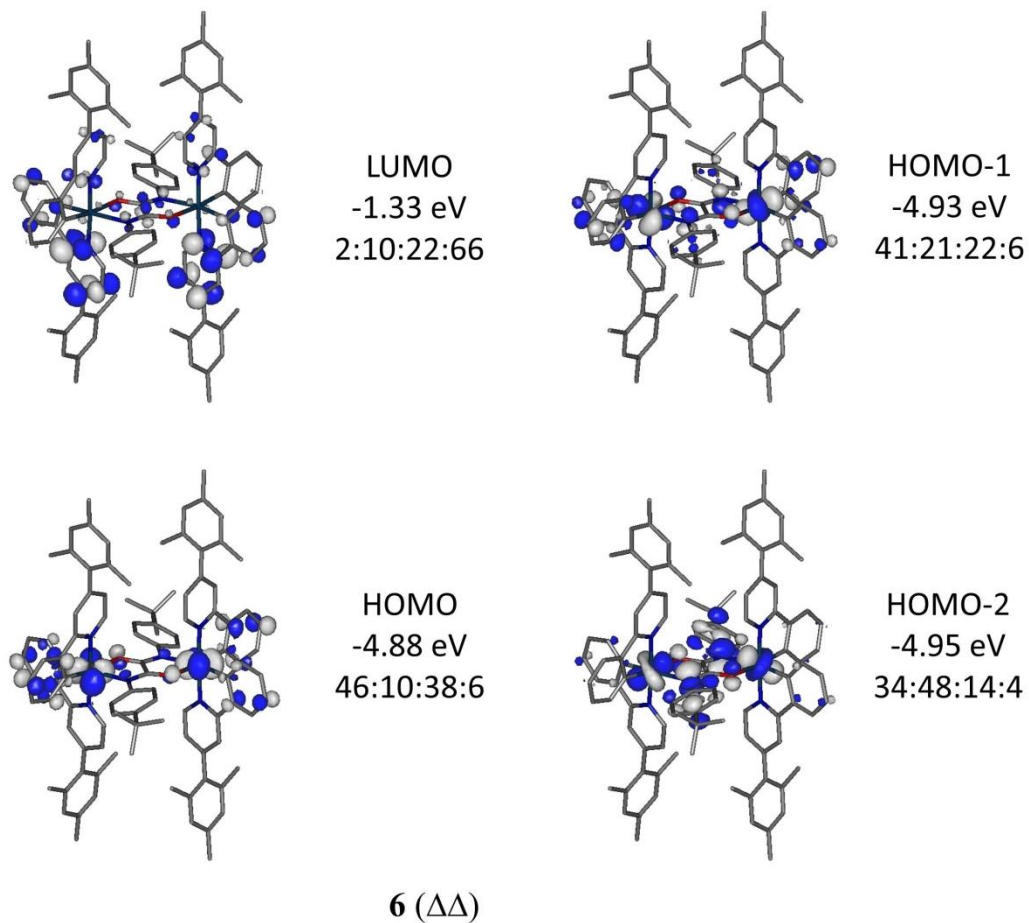


Figure S5. Important orbitals for **6(ΔΔ)**. Contour values are plotted at ± 0.035 e bohr⁻³. The Ir:bridge:phenyl:pyridyl ratios represent the atom/group MO contributions in percentages.

Table S2. Selected bond distances in Å for computed and experimental geometries of complexes **2**, **4**, **5** and **6**.

	2 ($\Delta\Delta$)	2 ($\Delta\Delta$)	4 ($\Delta\Delta$)	4 ($\Delta\Delta$)	5 ($\Delta\Delta$)	5 ($\Delta\Delta$)	6 ($\Delta\Delta$)	6 ($\Delta\Delta$)
	calc	expt ^a	calc	expt ^b	calc	expt	calc	expt
Ir-N(3)(OPy)	2.043	2.030(5)	2.063	2.048(13) 2.025(13)	2.042	2.042(3)	2.047	2.023(4)
Ir-N(4)(NPy)	2.058	2.029(5)		2.052(13) 2.027(13)	2.058	2.032(3)	2.058	2.040(4)
Ir-C(1)(OPh)	2.010	1.993(5)	2.011	1.992(17)	2.009	1.993(4)	2.017	1.982(4)
Ir-C(12)(NPh)	2.029	2.008(6)		2.03(2)	2.029	2.013(3)	2.020	2.013(4)
Ir-O(1)	2.212	2.20(2)			2.209	2.194(13)	2.163	2.184(3)
Ir-O(2)		2.180(15)				2.19(2)		
Ir-N(1)(br)	2.154	2.18(2)			2.152	2.13(2)	2.247	2.147(3)
Ir-N(2)(br)		2.132(15)				2.135(18)		
N(1)-C(br)	1.315	1.30(2)			1.314	1.30(3)	1.332	1.309(5)
N(2)-C(br)		1.278(16)				1.307(19)		
O(1)-C(br)	1.305	1.30(2)			1.305	1.286(14)	1.305	1.269(5)
O(2)-C(br)		1.299(16)				1.28(3)		
C-C(br)	1.518	1.523(12)			1.517	1.526(7)	1.505	1.514(8)
Ir-Cl			2.597	2.529(5)				
Ir-Cl				2.529(4)				
Ir...Ir ²	5.781	5.718	3.944	3.812	5.775	5.688	5.829	5.726

^aM. Graf, R. Czerwieniec and K. Sünkel, *Zeit. Anorg. Allg. Chem.*, 2013, **639**, 1090–1094.

^bD. Rota Martir, C. Momblona, A. Pertegás, D. B. Cordes, A. M. Z. Slawin, H. J. Bolink and E. Zysman-Colman, *ACS Appl. Mater. Interfaces*, 2016, **8**, 33907–33915.

Table S3. Orbital energies and % MO contributions for **4** ($\Delta\Delta$).

	eV	Symmetry	Ir	Cl	Ph	Py	Mes
LUMO +5	-0.84	A	0	0	12	86	2
LUMO +4	-0.94	B ₃	2	0	10	86	2
LUMO +3	-1.21	B ₂	6	1	22	69	2
LUMO +2	-1.31	A	6	1	18	73	2
LUMO +1	-1.36	B ₃	4	1	24	69	2
LUMO	-1.37	B ₁	8	1	26	63	2
HOMO	-4.91	A	44	6	44	6	0
HOMO -1	-4.98	B ₂	49	1	44	6	0
HOMO -2	-5.41	B ₃	62	18	8	12	0
HOMO -3	-5.47	B ₂	62	18	10	10	0
HOMO -4	-5.70	B ₁	52	2	26	20	0
HOMO -5	-5.83	A	69	1	15	15	0

Table S4. Orbital energies and % MO contributions for **5** ($\Delta\Delta$). NH = NHs at bridge, C₂ = carbons at bridge, NPh = phenyl *trans* to nitrogen at bridge, OPh = phenyl *trans* to oxygen at bridge, NPy = pyridyl group of ppy with NPh, OPy = pyridyl group of ppy with OPh.

	eV	Symmetry	Ir	NH	O	C ₂	NPh	OPh	NPy	OPy	Mes
LUMO +4	-0.82	A _u	2	2	1	2	6	6	36	43	2
LUMO +3	-1.18	A _u	6	0	0	0	10	10	37	35	2
LUMO +2	-1.21	A _g	6	0	0	0	10	8	42	32	2
LUMO +1	-1.27	A _g	4	0	0	0	10	14	31	39	2
LUMO	-1.33	A _u	5	0	0	1	12	12	34	34	2
HOMO	-4.79	A _g	45	2	6	1	20	20	4	2	0
HOMO -1	-4.84	A _u	45	1	2	0	22	22	4	4	0
HOMO -2	-5.06	A _g	57	16	11	0	4	2	4	6	0
HOMO -3	-5.23	A _u	57	10	14	1	4	4	4	6	0
HOMO -4	-5.61	A _g	69	0	2	2	8	4	11	4	0
HOMO -5	-5.67	A _u	47	0	0	2	19	12	12	8	0

Table S5. Orbital energies and % MO contributions for **5** ($\Delta\Delta$).

	eV	Symmetry	Ir	NH	O	C ₂	NPh	OPh	NPy	OPy	Mes
LUMO +4	-0.83	A	4	3	2	3	4	4	38	40	2
LUMO +3	-1.19	B	4	0	0	0	10	12	37	35	2
LUMO +2	-1.24	A	6	0	0	0	10	10	40	32	2
LUMO +1	-1.27	B	6	0	0	0	12	12	34	34	2
LUMO	-1.29	A	4	1	1	1	12	14	30	35	2
HOMO	-4.80	A	47	1	5	1	22	20	2	2	0
HOMO -1	-4.83	B	45	1	2	0	22	22	4	4	0
HOMO -2	-5.10	B	57	15	11	1	4	2	4	6	0
HOMO -3	-5.27	A	59	10	15	1	3	4	4	4	0
HOMO -4	-5.61	B	67	1	2	2	8	6	10	4	0
HOMO -5	-5.67	A	59	1	3	3	12	6	10	6	0

Table S6. Orbital energies and % MO contributions for **6** ($\Delta\Delta$). Bu = tBuC₆H₄ group.

	eV	Symmetry	Ir	N	O	C ₂	Bu	NPh	OPh	NPy	OPy	Mes
LUMO +6	-0.81	A _u	0	1	2	3	2	10	4	60	16	2
LUMO +5	-0.82	A _g	2	0	0	0	0	12	2	76	6	2
LUMO +4	-1.08	A _u	4	17	15	28	24	0	0	6	6	0
LUMO +3	-1.21	A _u	6	0	0	0	0	6	16	20	50	2
LUMO +2	-1.23	A _g	6	1	0	0	1	2	20	8	60	2
LUMO +1	-1.32	A _g	4	0	1	0	0	20	4	61	8	2
LUMO	-1.38	A _u	4	1	1	3	2	16	6	49	16	2
HOMO	-4.82	A _g	39	9	7	1	18	10	12	2	2	0
HOMO -1	-4.91	A _u	47	2	2	0	3	18	22	2	4	0
HOMO -2	-4.96	A _g	39	11	6	1	15	8	14	2	4	0
HOMO -3	-5.14	A _u	35	11	18	2	22	2	6	2	2	0
HOMO -4	-5.65	A _g	70	0	2	2	2	6	6	6	6	0
HOMO -5	-5.73	A _u	31	1	0	0	10	18	22	4	14	0
HOMO -6	-5.75	A _g	2	1	1	0	3	41	36	8	8	0
HOMO -7	-5.77	A _g	28	5	4	1	38	8	8	2	6	0

Table S7. Orbital energies and % MO contributions for **6** ($\Delta\Delta$).

	eV	Symmetry	Ir	N	O	C ₂	Bu	NPh	OPh	NPy	OPy	Mes
LUMO +6	-0.79	B	2	0	0	0	0	8	6	43	39	2
LUMO +5	-0.80	A	2	1	1	3	2	8	4	55	22	2
LUMO +4	-1.11	A	4	15	15	27	23	0	0	8	8	0
LUMO +3	-1.23	B	4	0	0	0	0	8	16	22	48	2
LUMO +2	-1.27	A	6	1	0	0	0	4	18	14	55	2
LUMO +1	-1.30	B	6	0	0	0	0	16	8	46	22	2
LUMO	-1.33	A	2	2	2	3	3	18	4	52	12	2
HOMO	-4.88	A	46	2	4	1	3	17	21	2	4	0
HOMO -1	-4.93	B	41	6	4	1	10	12	20	2	4	0
HOMO -2	-4.95	B	34	14	6	2	26	8	6	2	2	0
HOMO -3	-5.18	A	37	11	18	2	22	2	4	2	2	0
HOMO -4	-5.64	B	67	1	2	2	2	6	6	8	6	0
HOMO -5	-5.72	A	38	4	5	1	4	20	18	4	6	0
HOMO -6	-5.78	A	18	0	0	0	4	30	28	8	12	0
HOMO -7	-5.78	B	6	0	0	0	6	36	34	8	10	0

Table S8. TD-DFT data from optimised geometries of the complexes, **1**, **2**, **4**, **5** and **6** and comparison with observed lowest energy absorption bands and emission maxima.

	TD-DFT $S_0 \rightarrow S_1$ (nm)	Oscillator strength (<i>f</i>)	TD-DFT $S_0 \rightarrow T_1$ (nm)	Observed λ_{abs} (nm)	Observed λ_{em} (nm)	Observed Stokes shift (cm^{-1})
1 ($\Delta\Lambda$)	476	0.0112	506	497 ^a	521 ^a	930
1 ($\Delta\Delta$)	470	0.0200	498	497 ^a	523 ^a	1000
2 ($\Delta\Lambda$)	449	0.0405	488	498 ^b	523 ^b	960
2 ($\Delta\Delta$)	448	0.0409	490	498 ^b	523 ^b	960
4 ($\Delta\Delta$)	445	0.0685	485	492	518	1020
5 ($\Delta\Lambda$)	452	0.0673	490	500	529	1100
5 ($\Delta\Delta$)	448	0.0669	487	500	529	1100
6 ($\Delta\Lambda$)	449	0.0462	512	500	522	840
6 ($\Delta\Delta$)	441	0.0385	503	500	522	840

^a Y. Zheng, A. S. Batsanov, M. A. Fox, H. A. Al-Attar, K. Abdullah, V. Jankus, M. R. Bryce and A. P. Monkman, *Angew. Chem. Int. Ed.*, 2014, **53**, 11616–11619.

^b M. Graf, R. Czerwieńiec and K. Sünkel, *Zeit. Anorg. Allg. Chem.*, 2013, **639**, 1090–1094.

Mass spectra

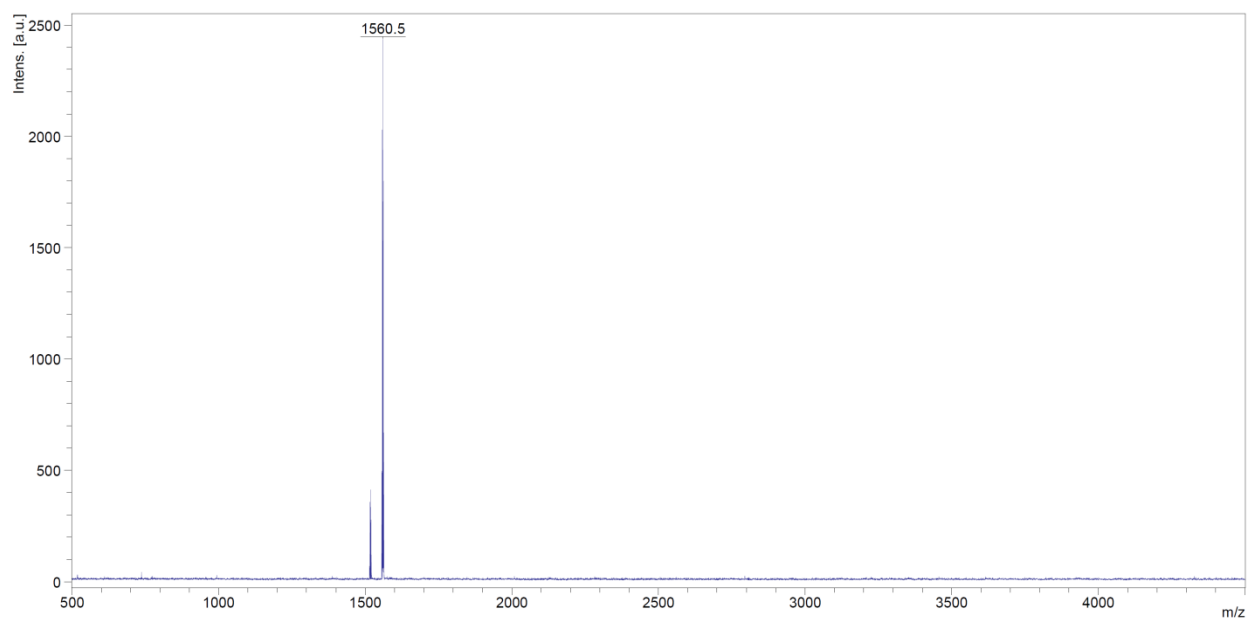


Figure S6. MALDI-TOF mass spectrum of complex **5**.

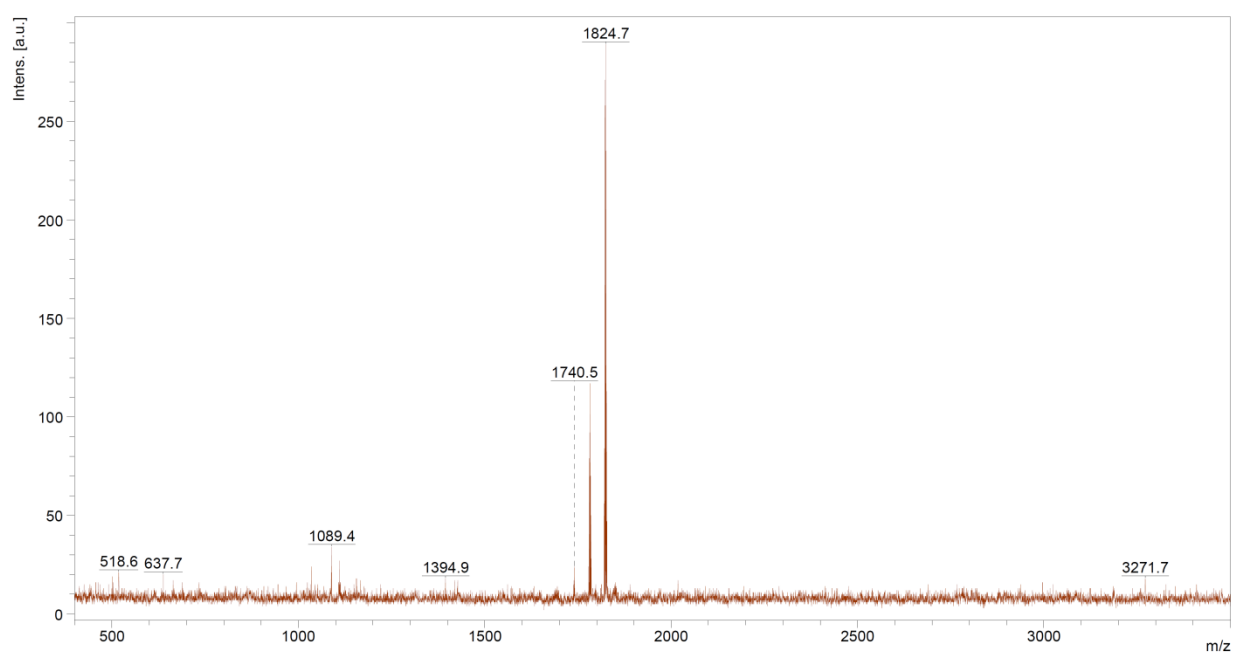


Figure S7. MALDI-TOF mass spectrum of complex **6**.

Thermal analysis

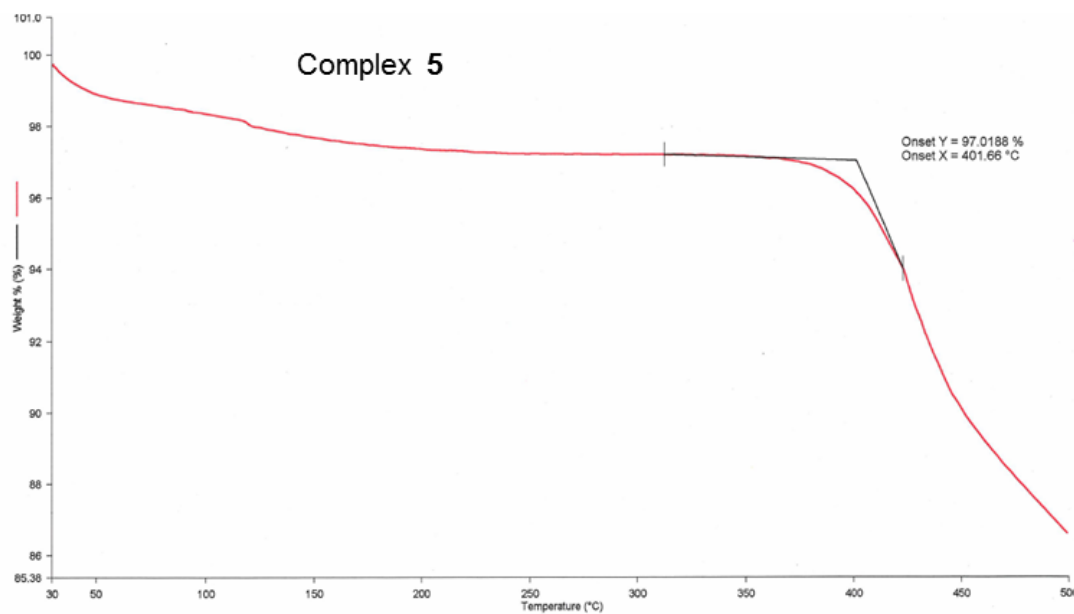


Figure S8. TGA trace of complex 5.

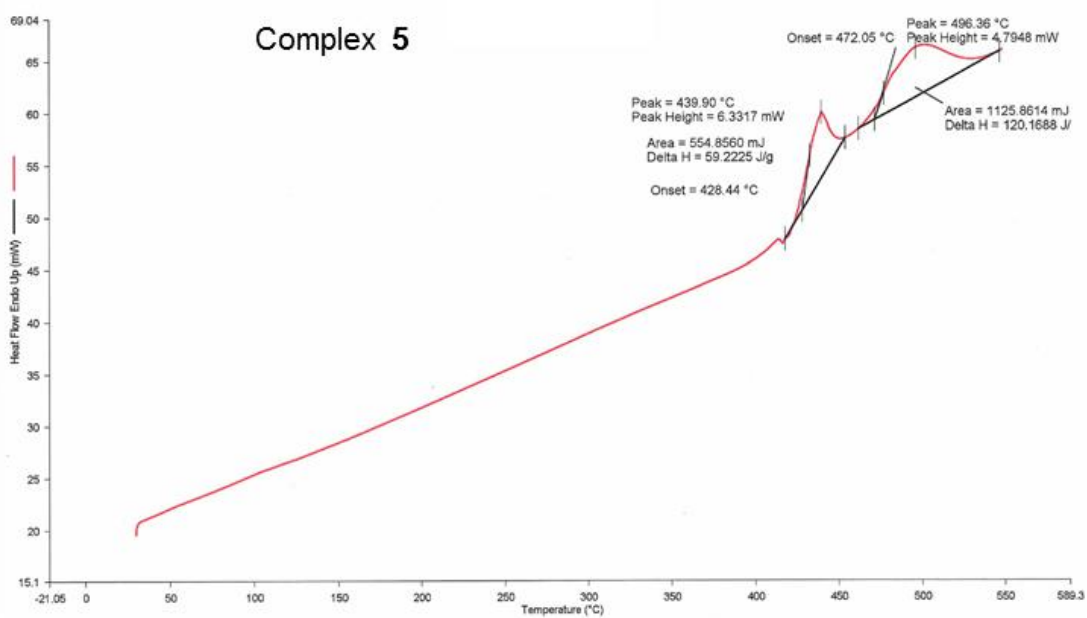


Figure S9. DSC trace of complex 5

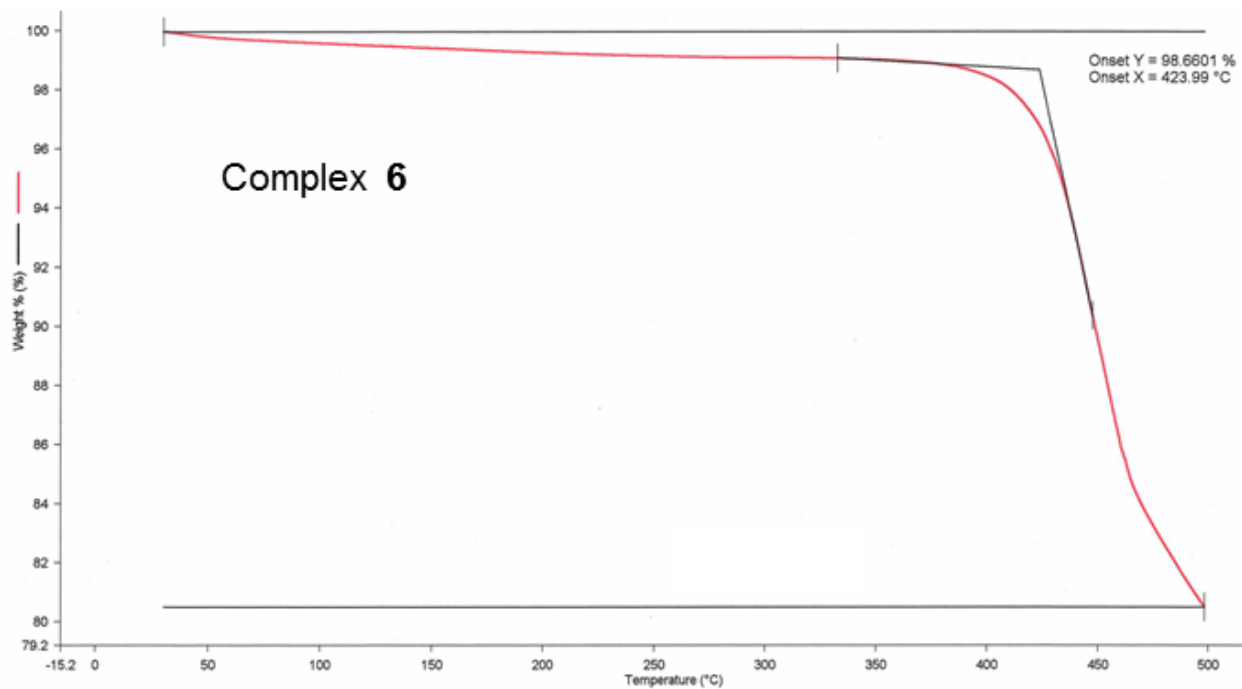


Figure S10. TGA trace of complex 6.

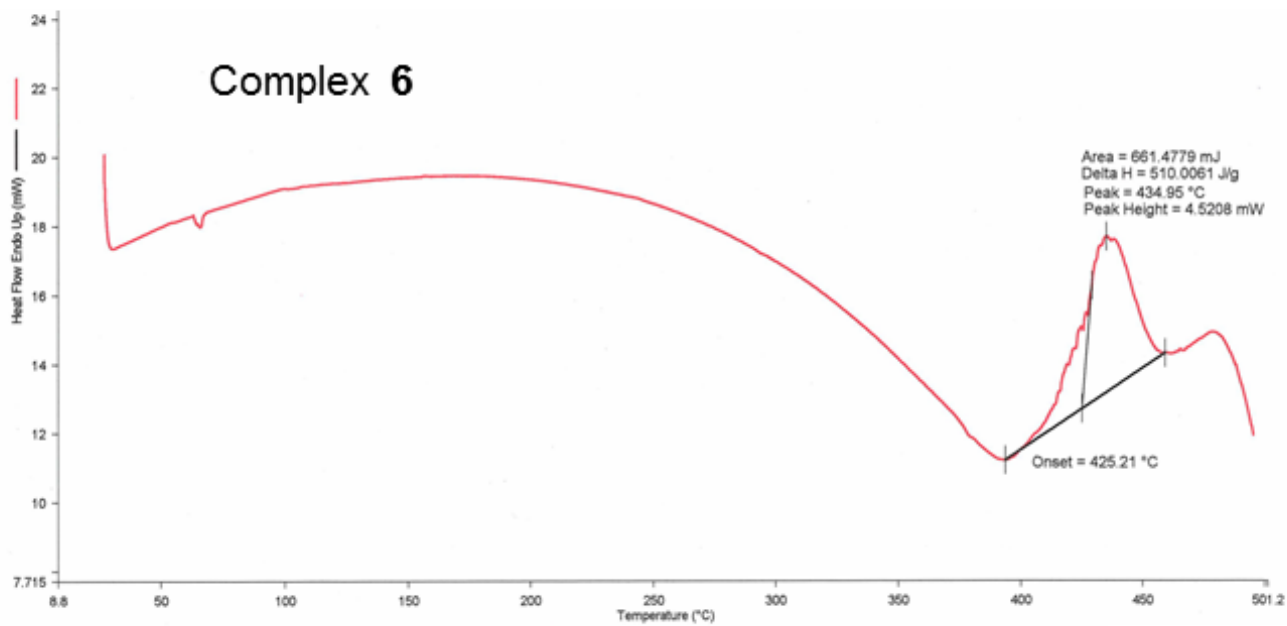


Figure S11. DSC trace of complex 6.

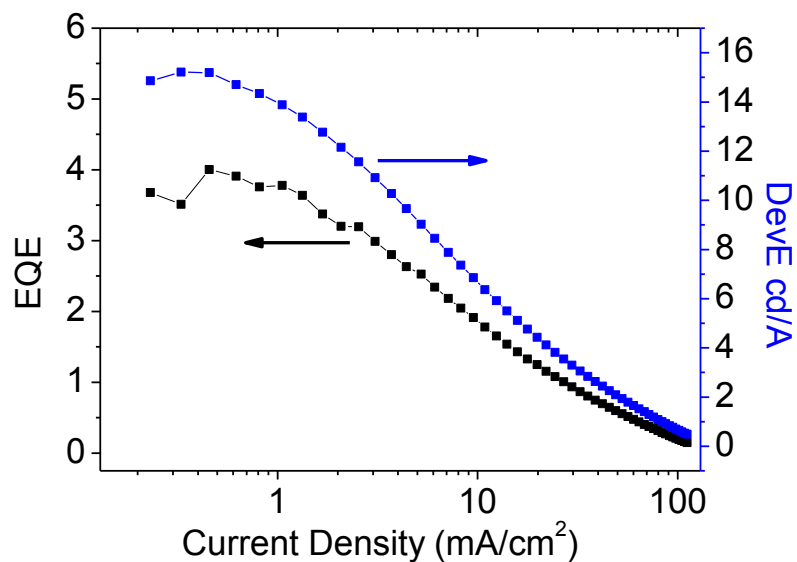
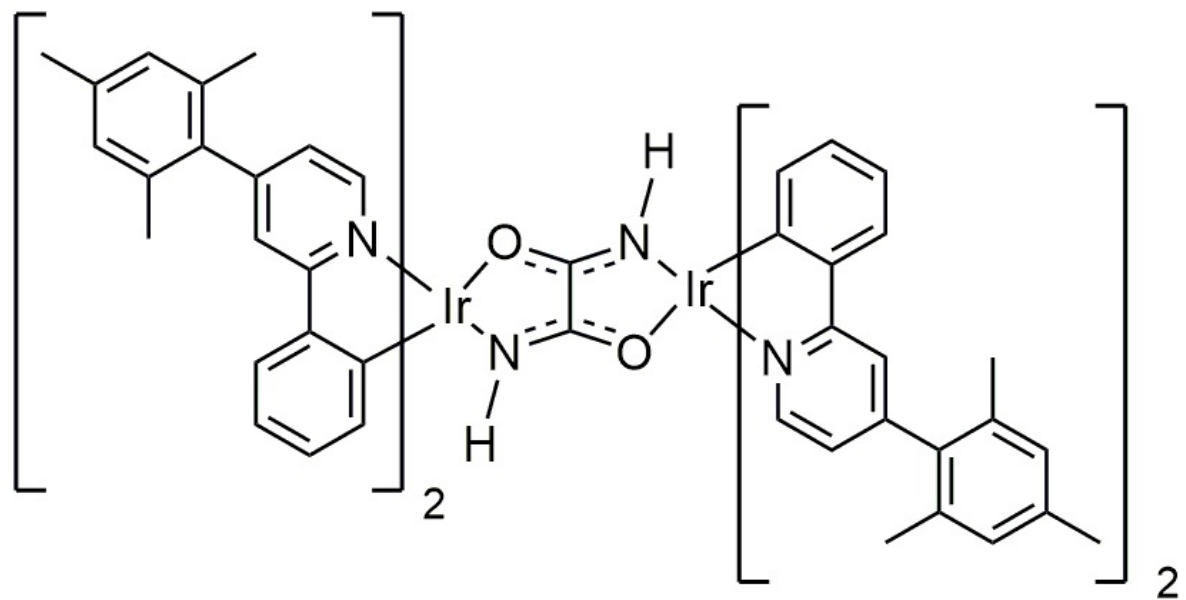
PhOLED data

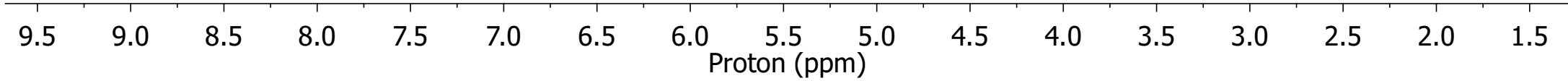
Figure S13. PhOLED data for complex **6** in low MWt PVK host with an additional spin-coated layer of TFB. Device structure: ITO/PEDOT:PSS (45 nm)/ TFB (60 nm)/ PVK:OXD-7(40%):Ir complex **6**(5%) (70 nm)/TPBi (30 nm)/LiF/Al.

NMR Spectra

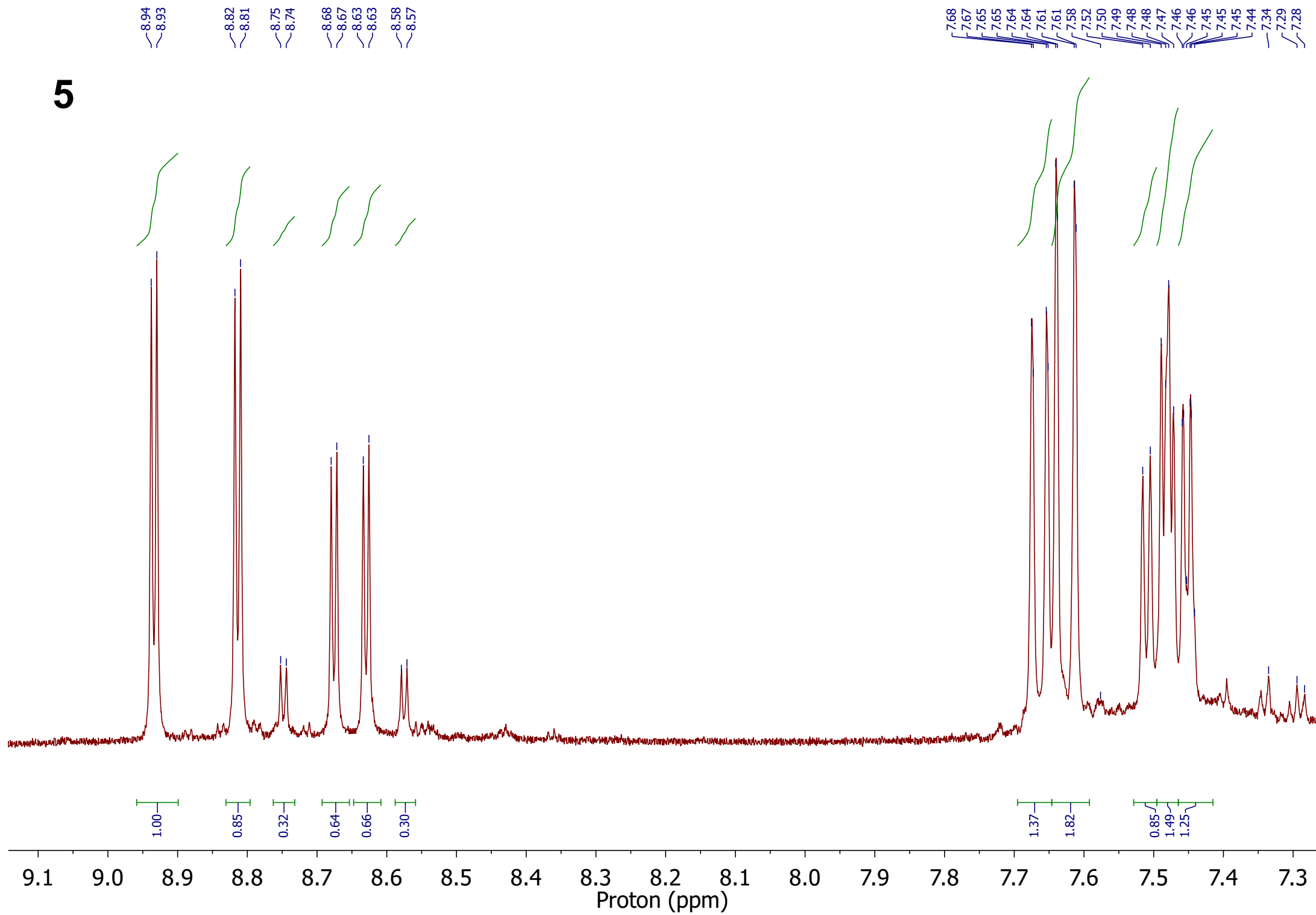
Residual CHCl₃ at
7.25 ppm in CDCl₃



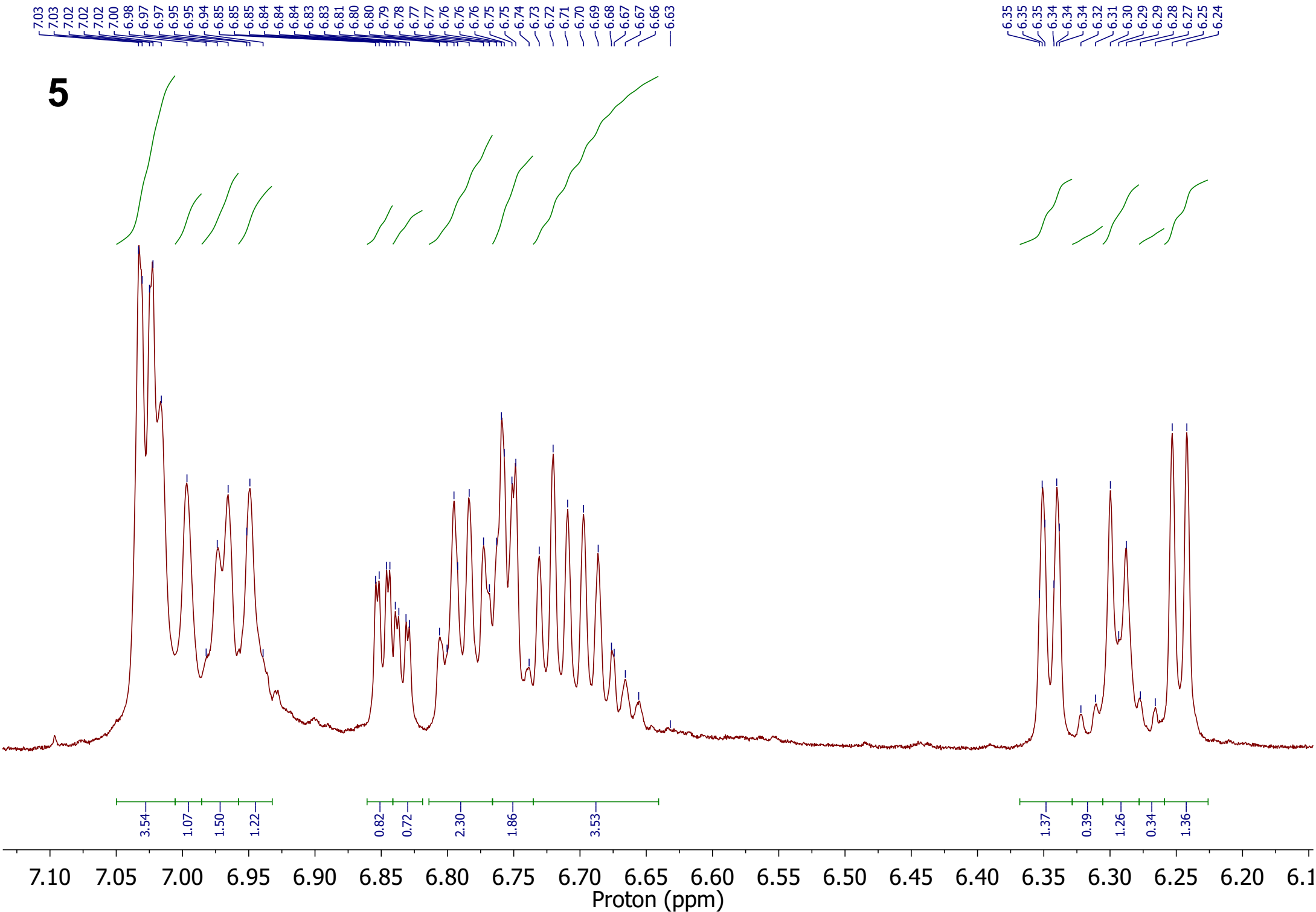
5



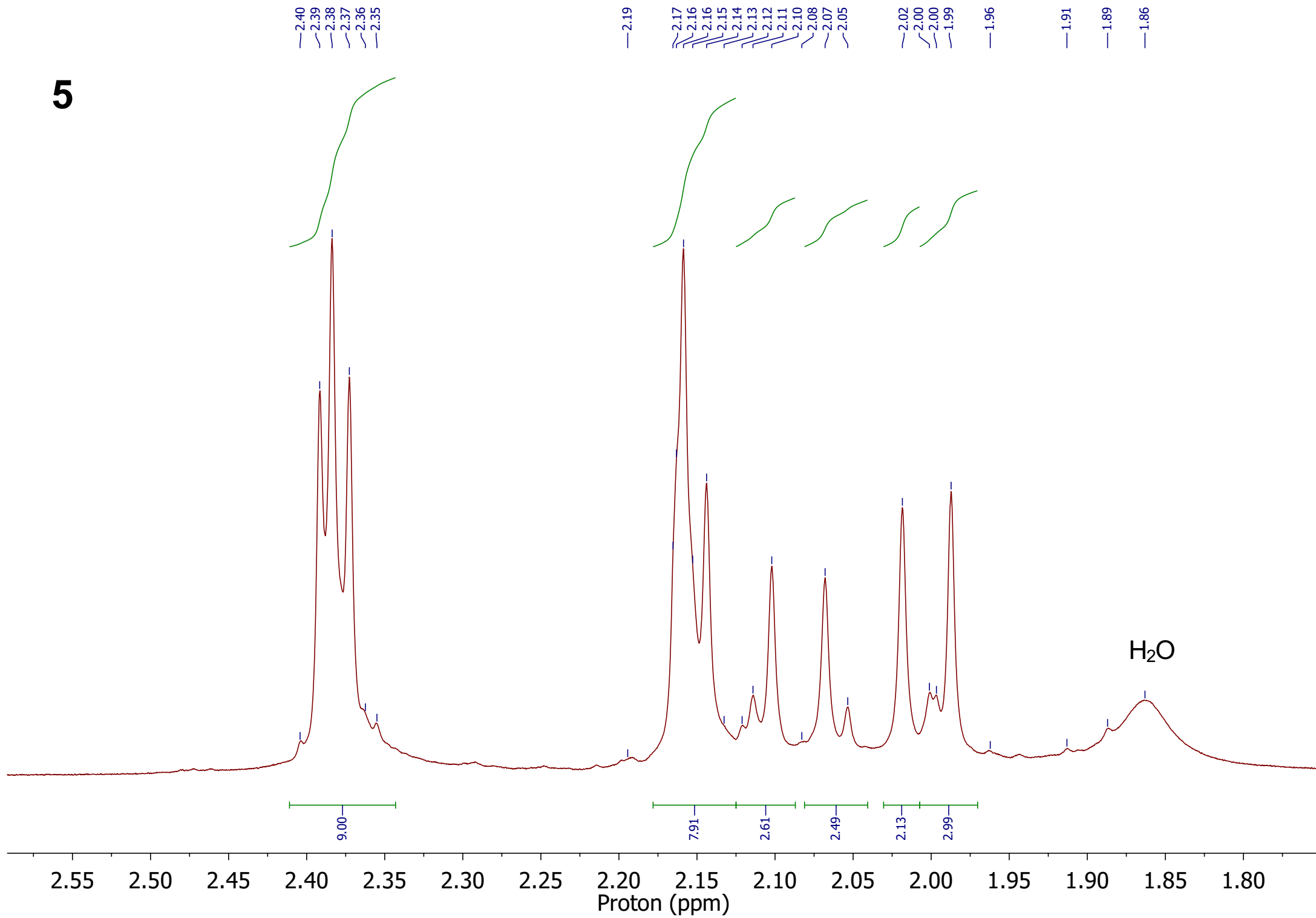
5

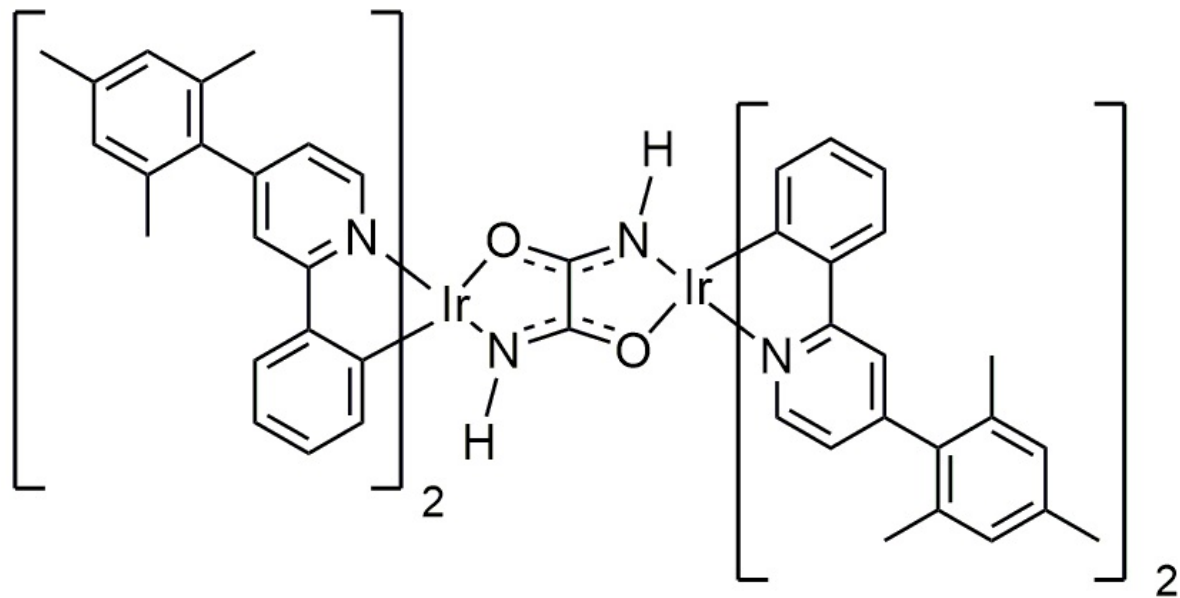


5



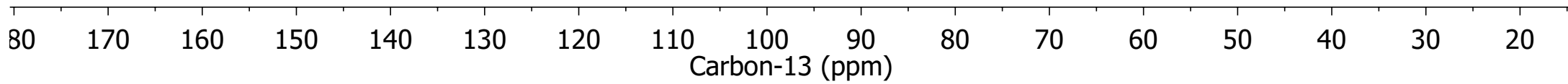
5





5

CDCl₃ at
77.00 ppm



5

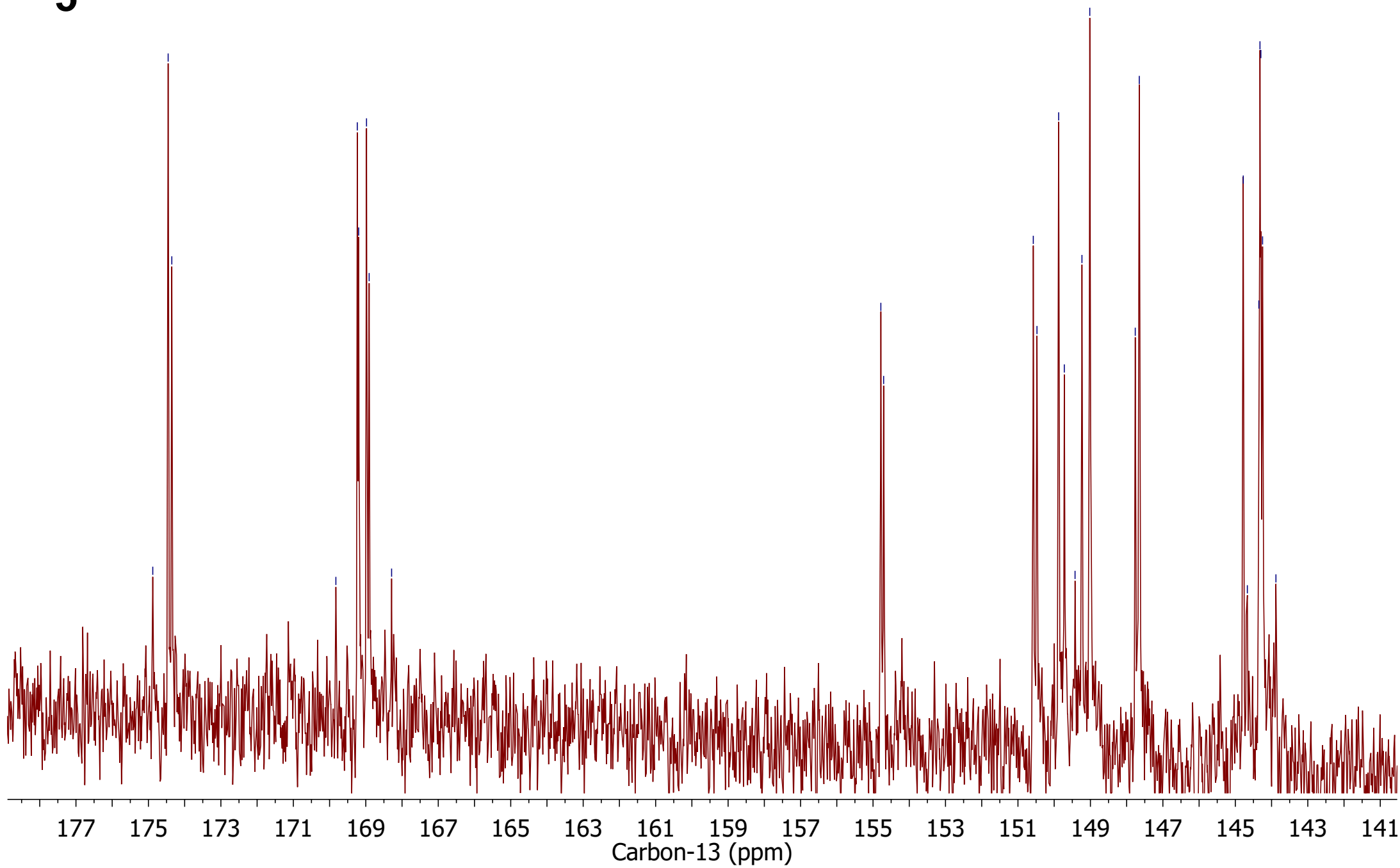
174.88
174.46
174.35

169.83
169.23
169.20
168.98
168.91
168.29

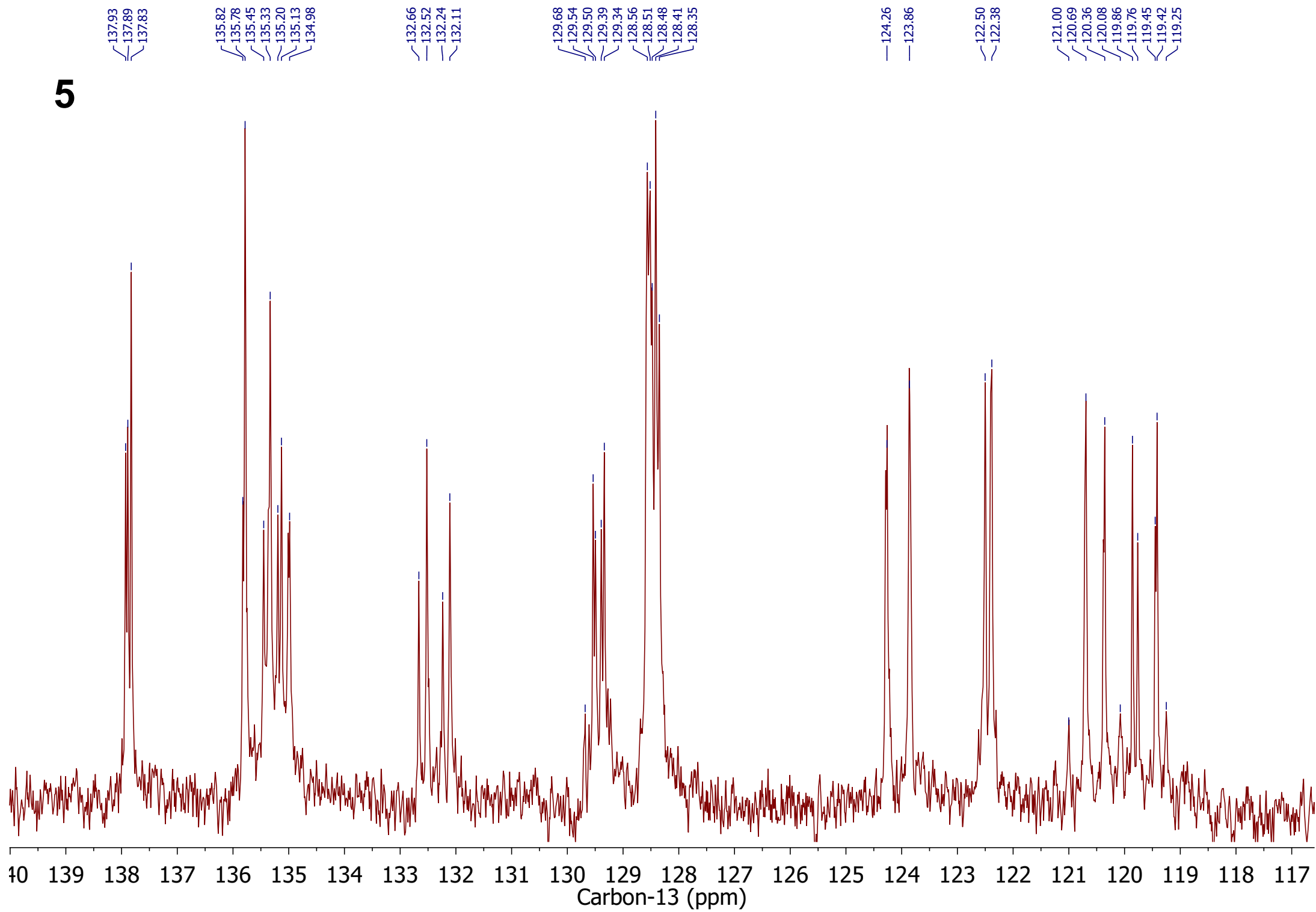
154.78
154.71

150.58
150.47
149.88
149.72
149.42
149.23
149.02
147.76
147.65

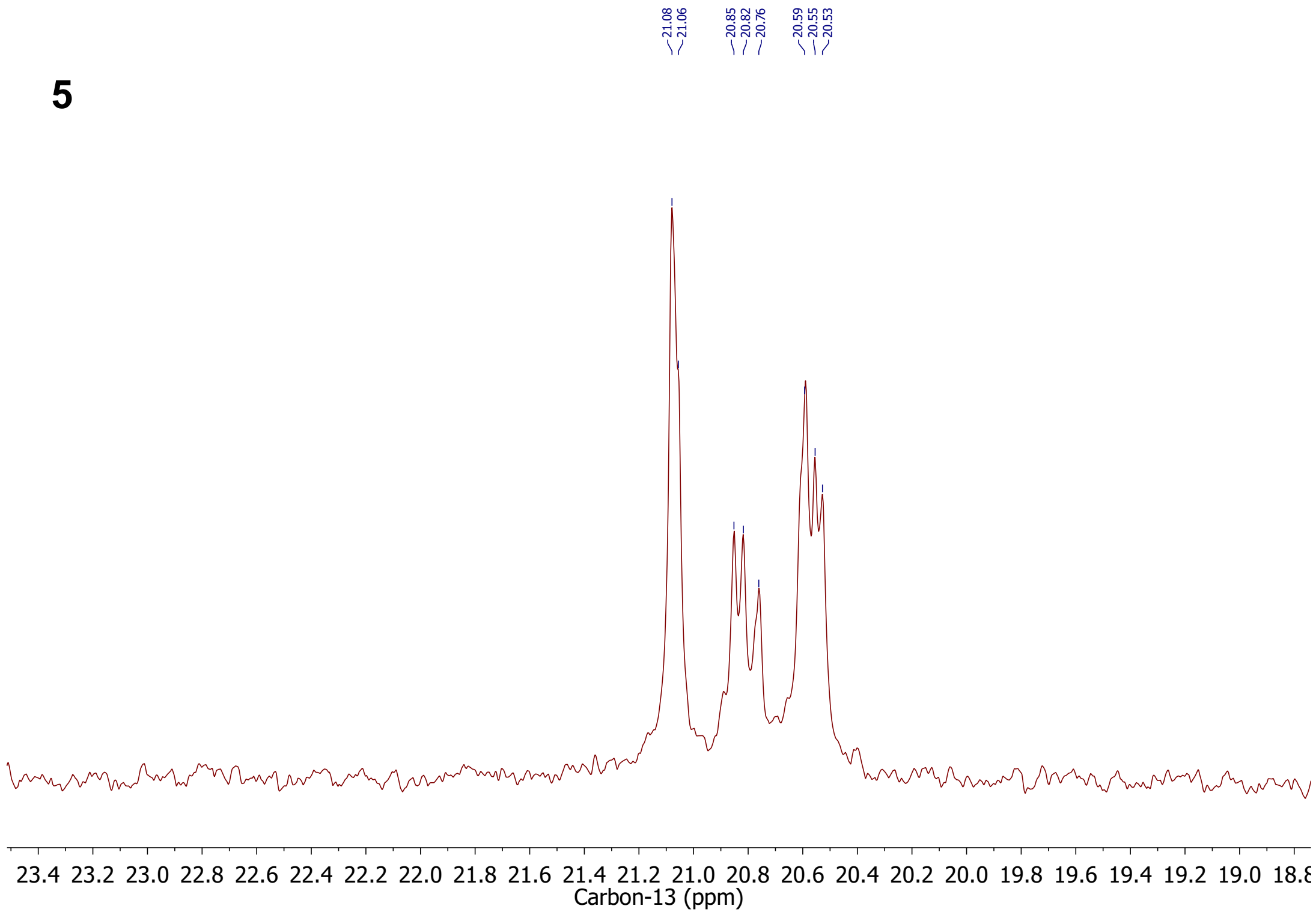
144.78
144.67
144.35
144.32
144.30
144.25
143.88

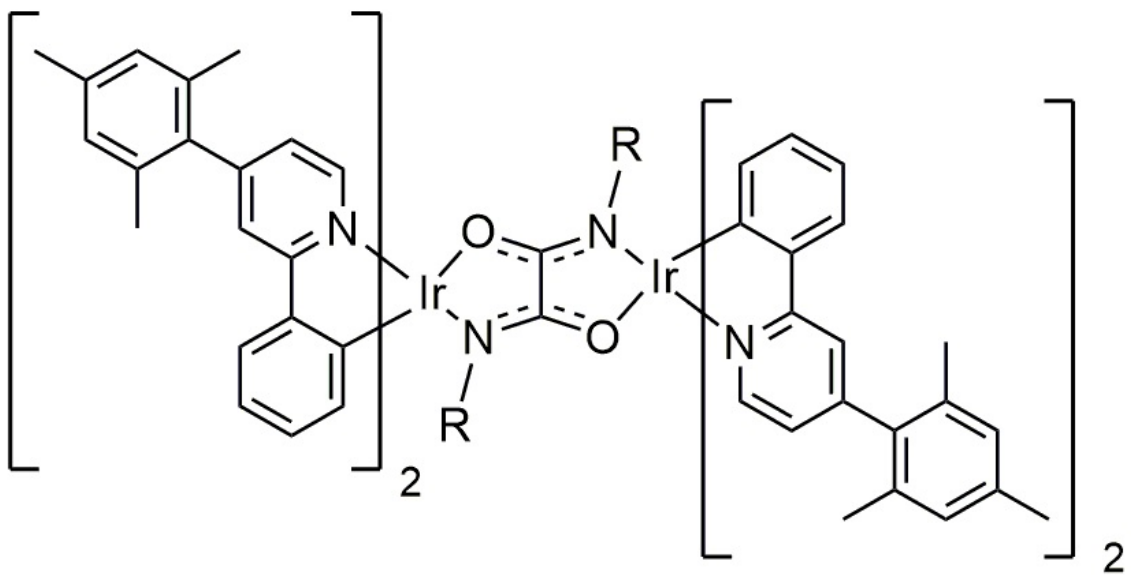


5

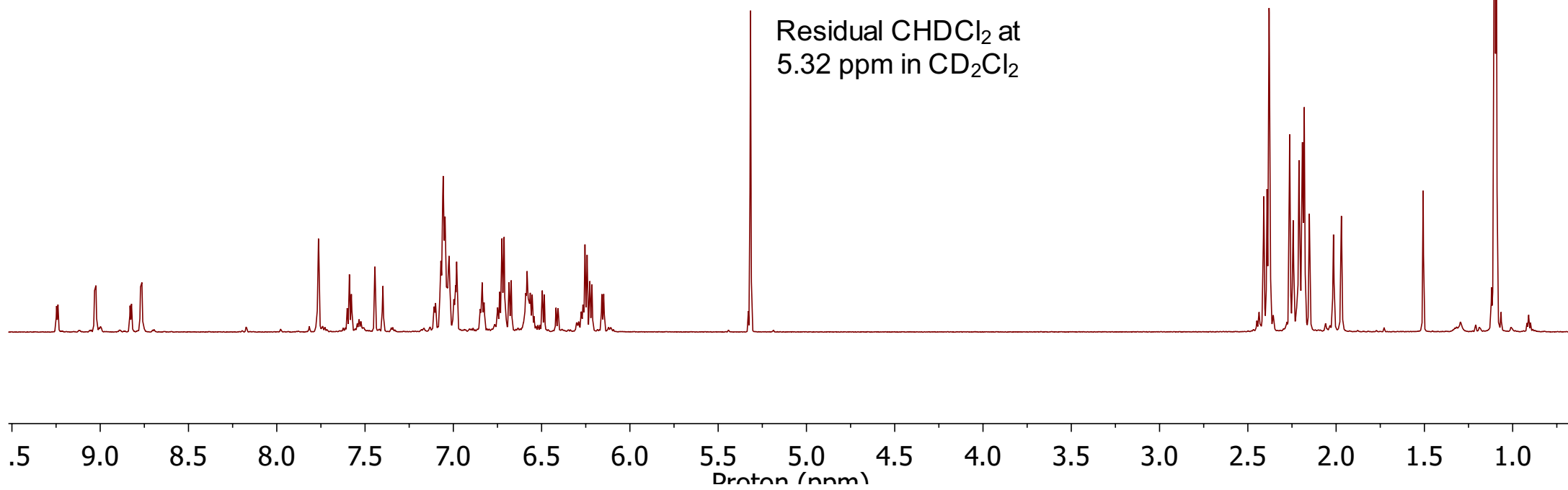


5

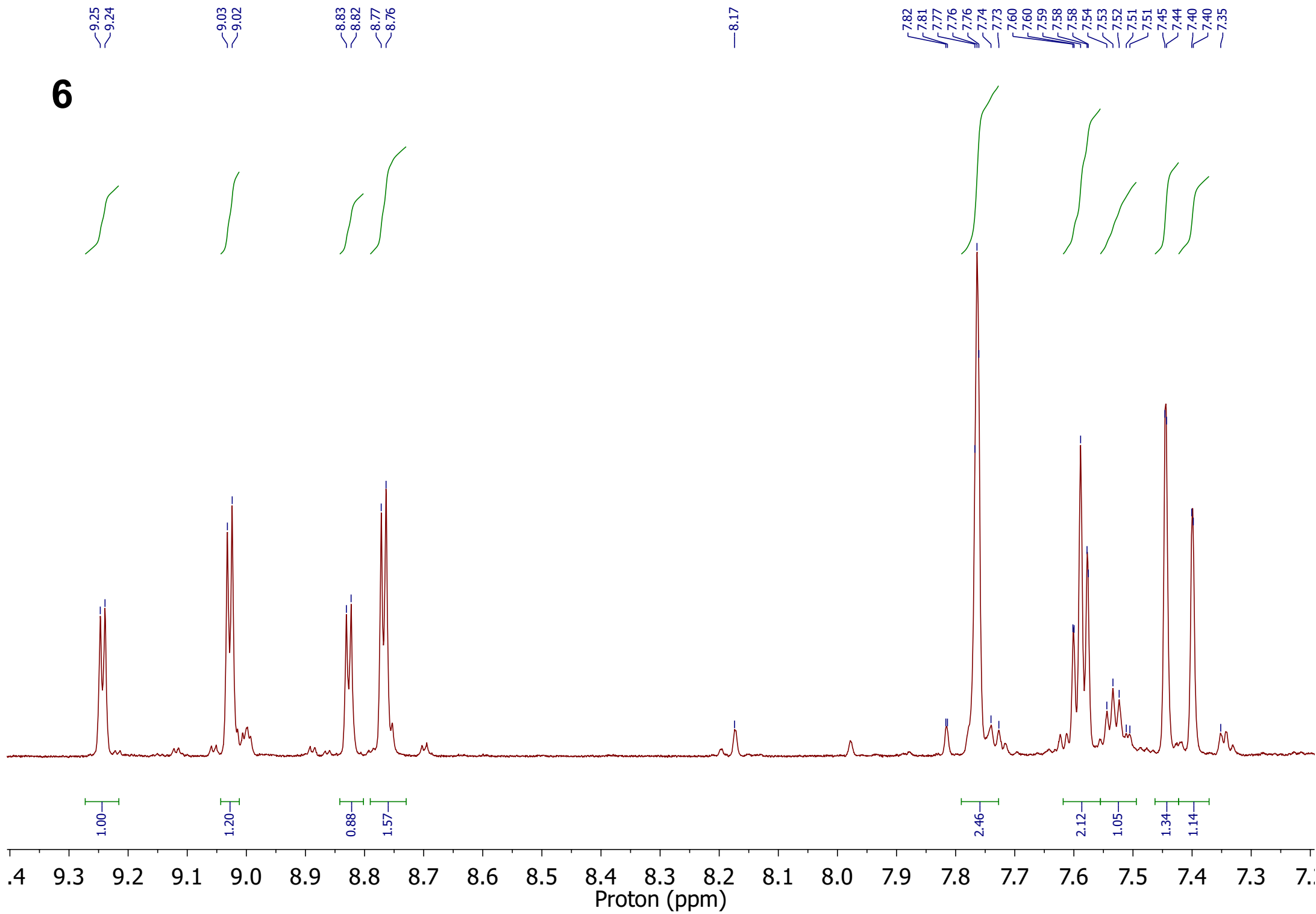




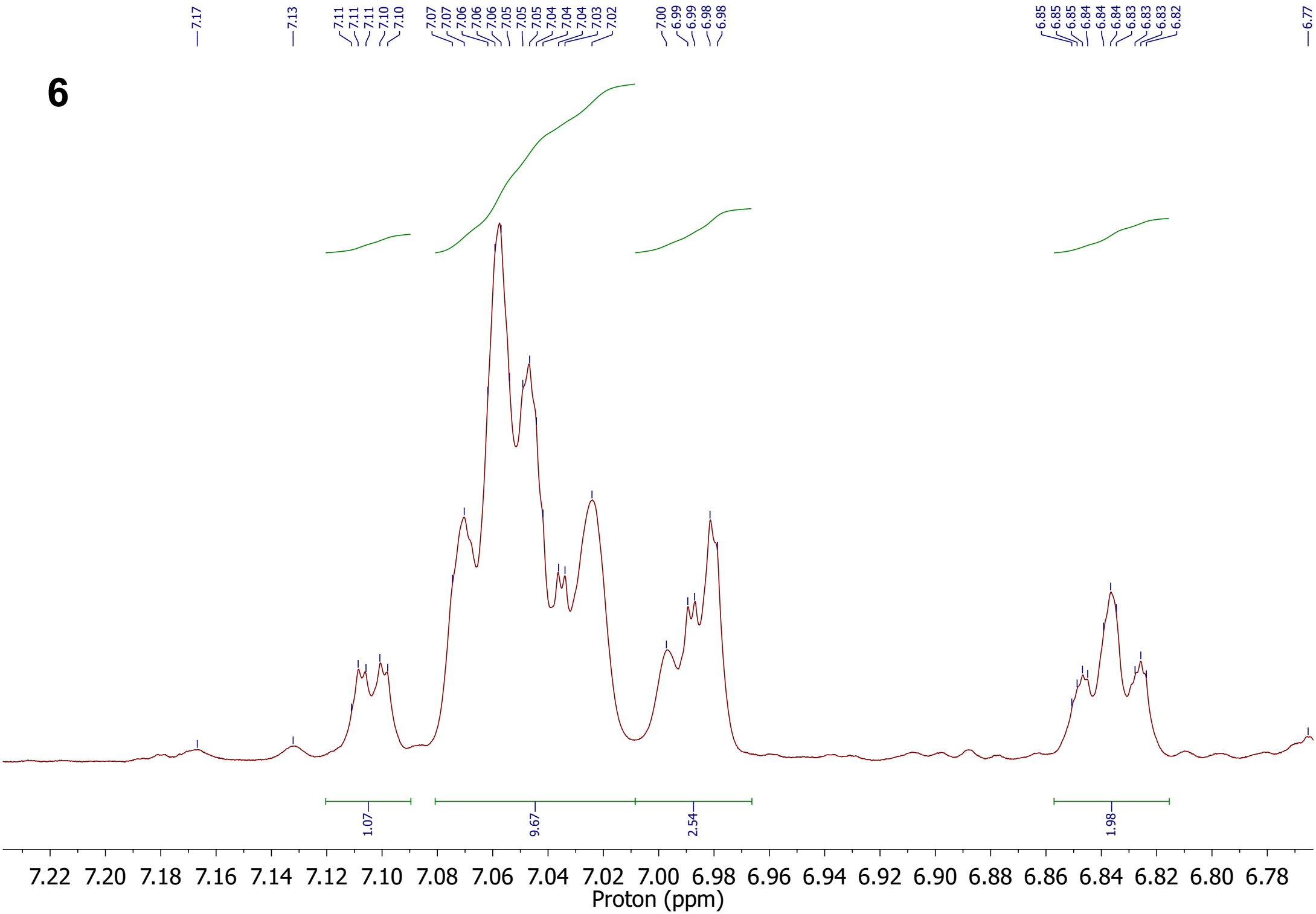
6 R = 4-*t*Bu-C₆H₄



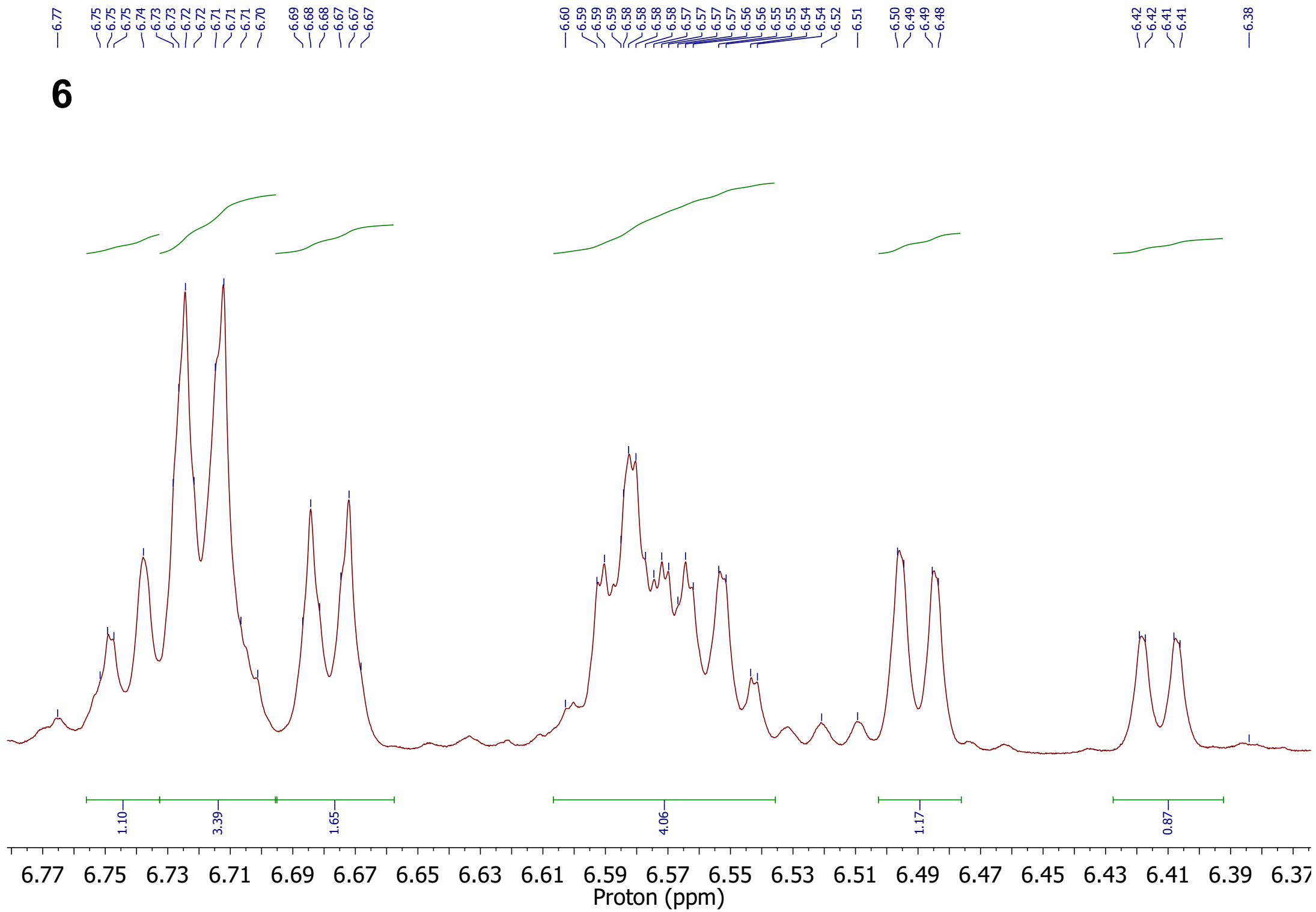
6



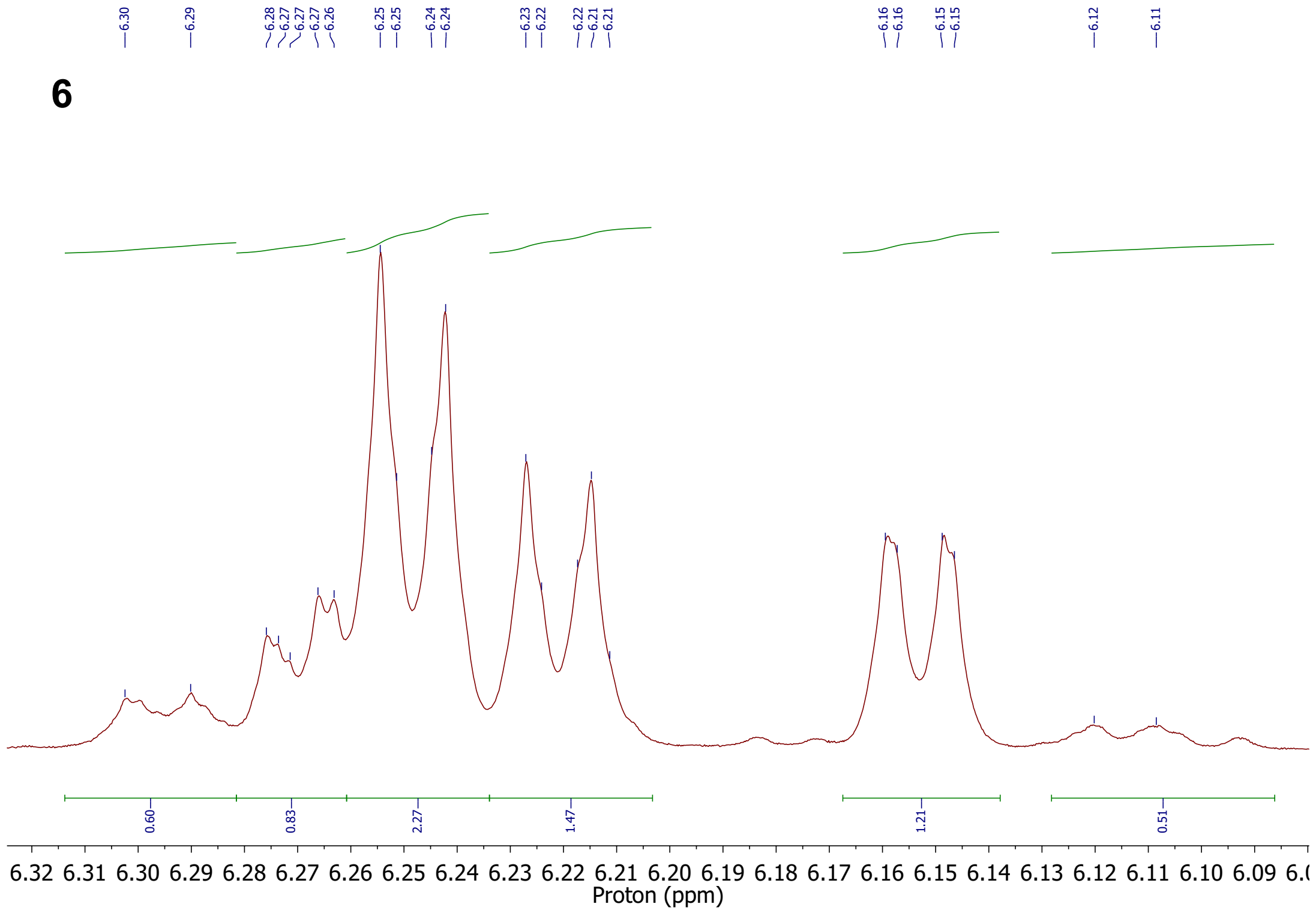
6



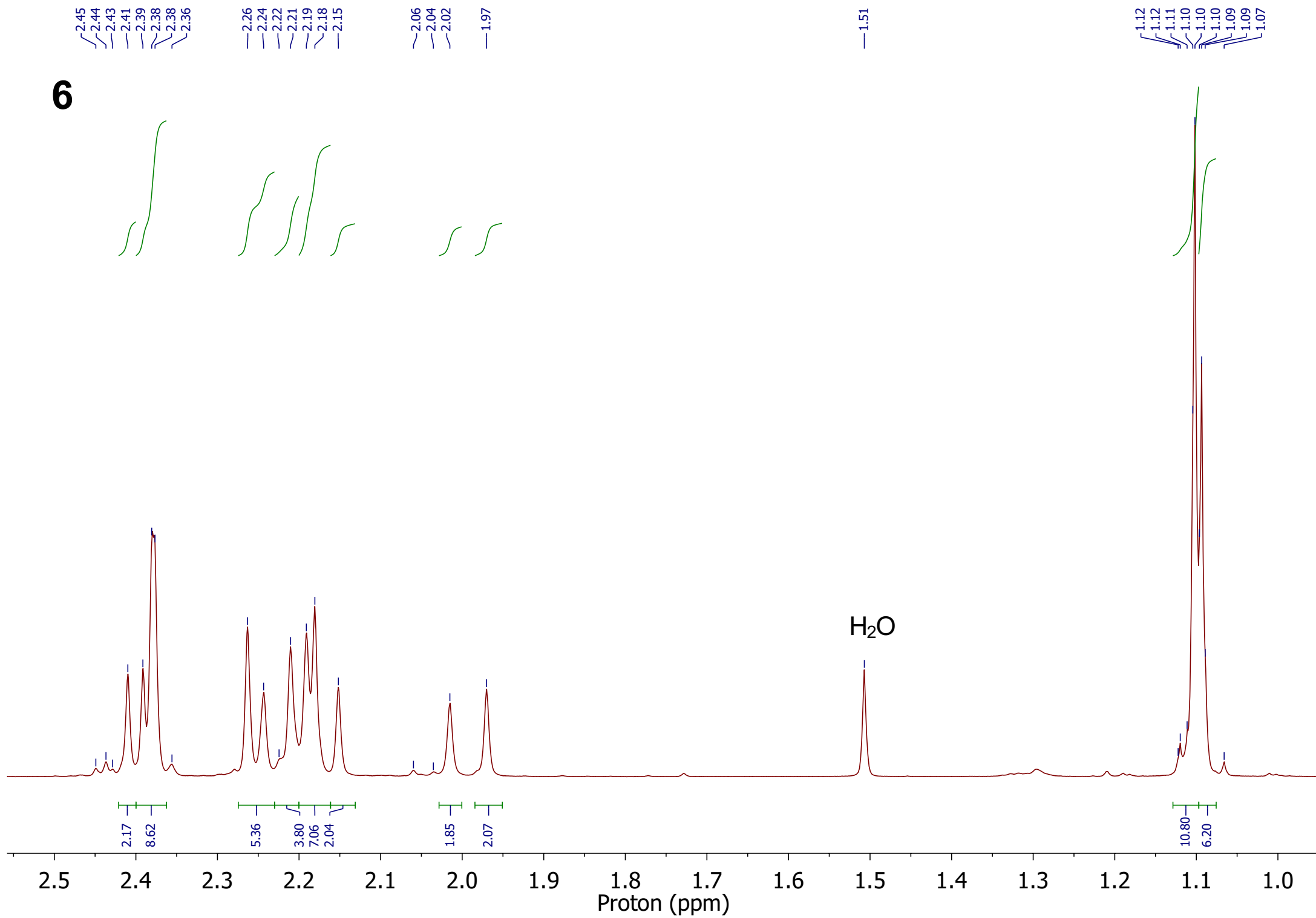
6

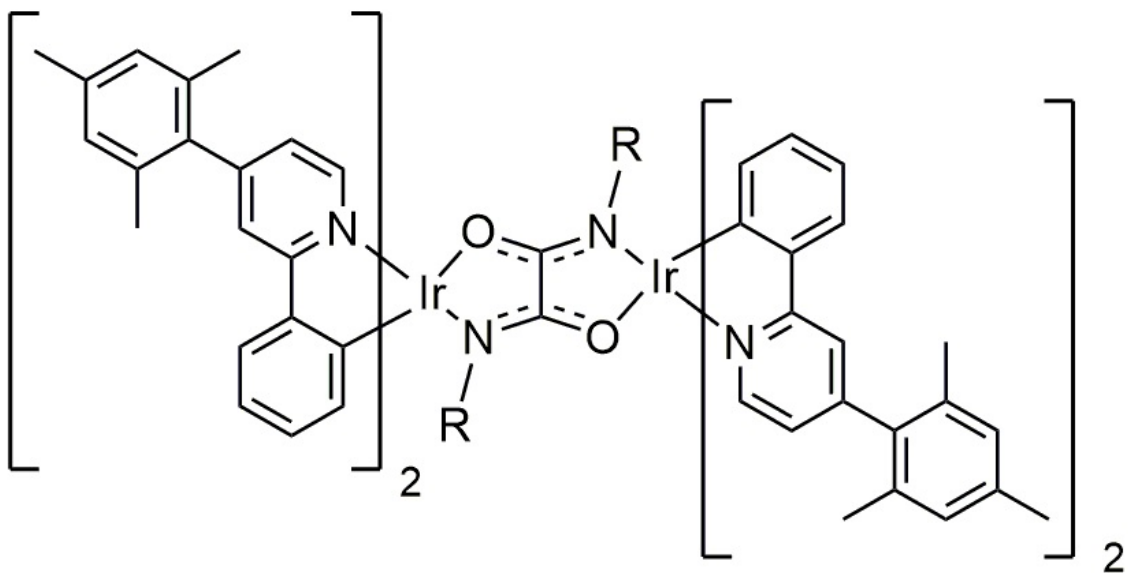


6



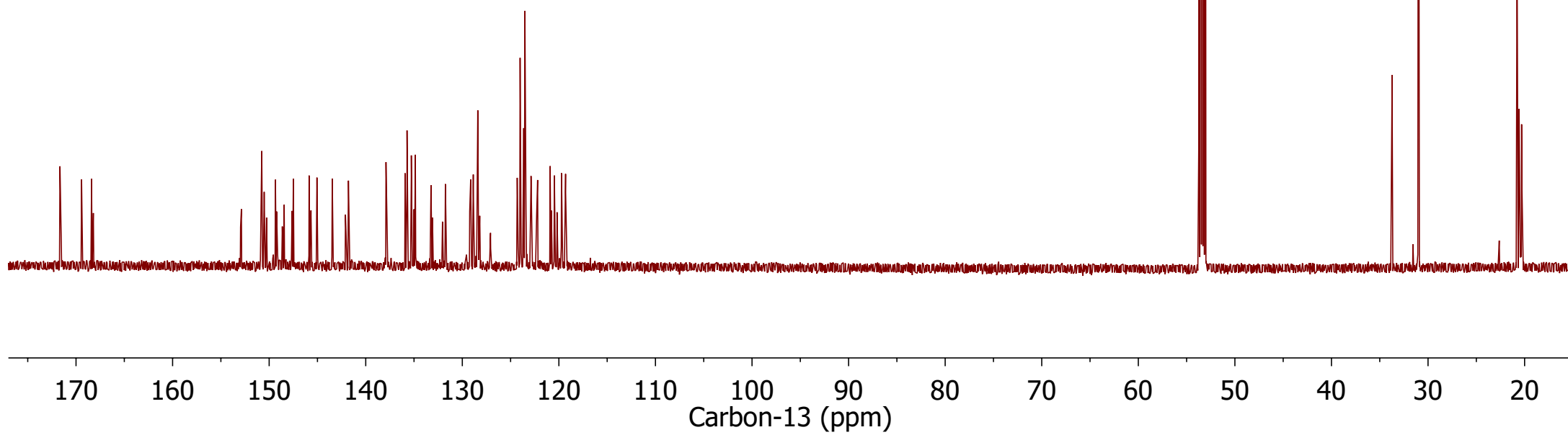
6



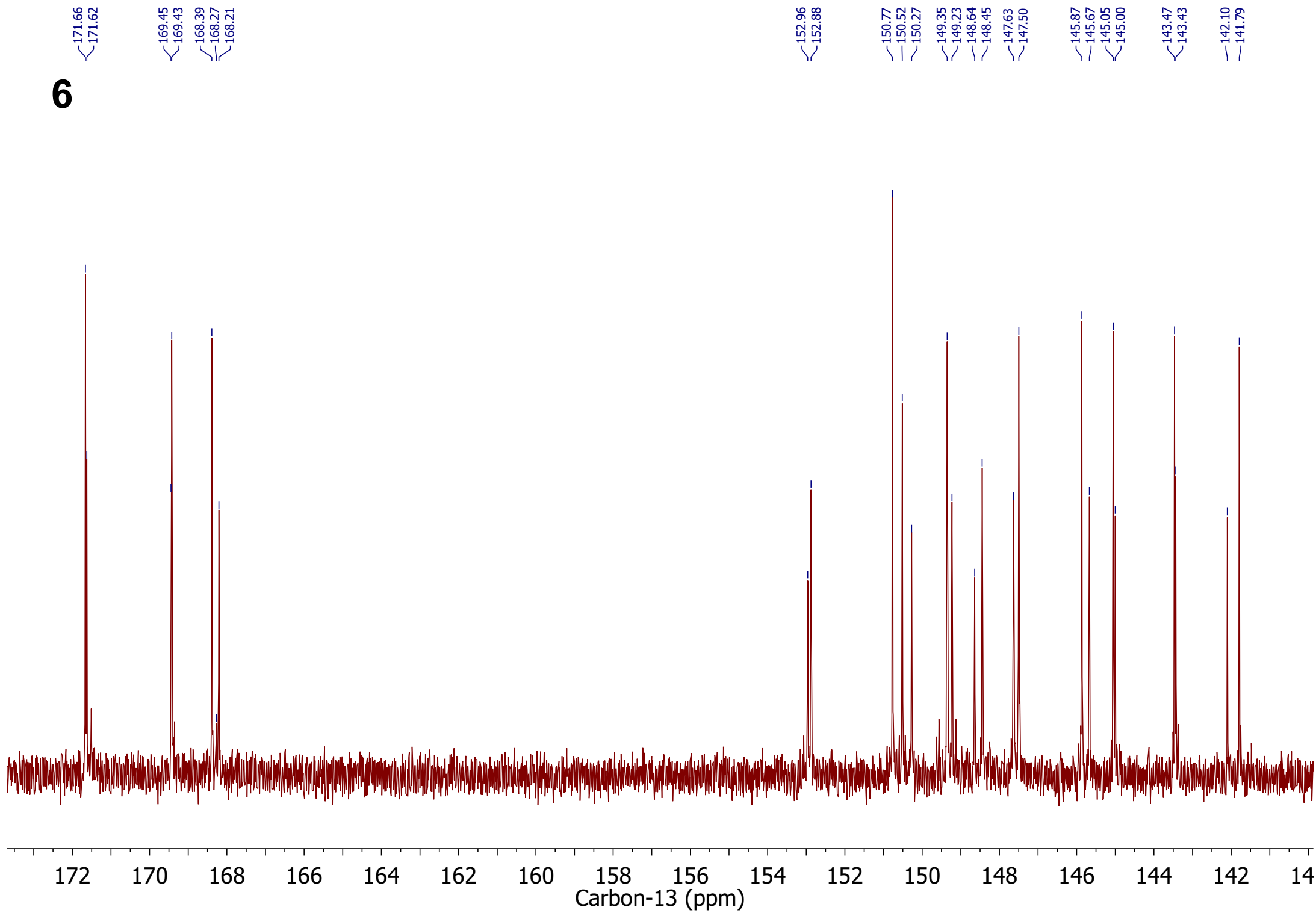


6 R = 4-*t*Bu-C₆H₄

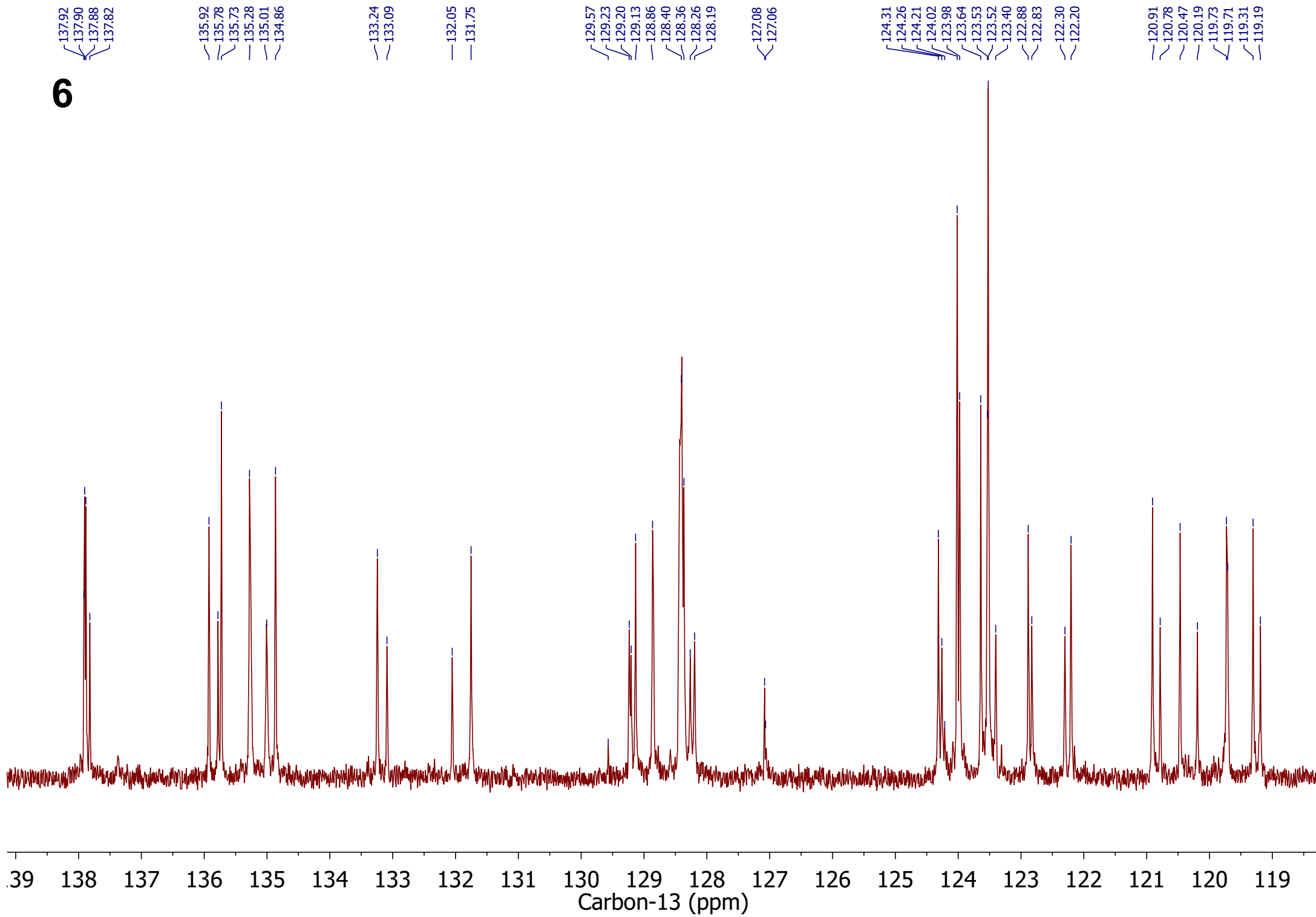
CD₂Cl₂ at
53.38 ppm



6



6



6

